The Eurasia Proceedings of Science, Technology, Engineering and Mathematics (EPSTEM)
ISSN: 2602-3199

The Eurasia Proceedings of Science, Technology, Engineering and Mathematics (EPSTEM), 2026

Volume 40, Pages 184-192

ICBAST 2026: International Conference on Basic Sciences and Technology

Pilot-Scale Laboratory Equipment for Agitated Gold Cyanidation

Nikolay Nestorov
University of Mining and Geology "St. Ivan Rilski"

Irena Grigorova
University of Mining and Geology "St. Ivan Rilski"

Abstract: Gold cyanidation remains the dominant hydrometallurgical technology for gold extraction, accounting for more than 78% of global production, despite persistent environmental and process-efficiency challenges. Although cyanidation chemistry is well established, a critical gap persists in the availability of pilot-scale laboratory systems capable of ensuring precise hydrodynamic control, regulated aeration, automated reagent dosing, and long-term operational stability required for reliable kinetic evaluation. This study presents the design, construction, and validation of a pilot-scale laboratory installation for agitated cyanidation of gold-bearing ores, concentrates, and tailings. The system integrates chemically resistant reactor materials, optimized propeller-driven mixing, controlled air dispersion, automated peristaltic reagent dosing, and vacuum-assisted sampling for continuous monitoring. A structured experimental program was conducted to determine optimal cyanide dosage, aeration rate, pulp density, pH control strategy, and leaching duration under stabilized process conditions. The installation enables continuous operation for up to 168 hours, multi-sample parallel testing, and minimal operator intervention while maintaining high reproducibility and operational stability. The results demonstrate that the system provides a robust experimental framework for kinetic evaluation and reagent optimization. The proposed configuration bridges the methodological gap between conventional laboratory testing and industrial cyanidation circuits, offering a scalable platform for advanced hydrometallurgical research.

Keywords: Gold, Cyanidation, Hydrometallurgy, Laboratory equipment, Process optimization

Introduction

The sustained expansion of advanced technologies has led to a continuous increase in global gold demand, reinforcing its strategic importance in electronics, aerospace systems, catalysis, green energy technologies, and high-precision manufacturing. This growing technological dependence necessitates the development of efficient, reliable, and economically sustainable gold extraction processes. In primary gold-bearing ores, gold predominantly occurs as native gold (Au) and electrum (Au, Ag), and less frequently as gold and gold-silver tellurides. Depending on mineralogical characteristics, beneficiation strategies typically involve gravity concentration, flotation, cyanidation, or integrated flowsheets combining these methods (Badri & Zamankhan, 2013; Li et al., 2023).

For more than 130 years, cyanidation - known as the MacArthur-Forrest process has remained the dominant industrial technology for gold extraction, accounting for over 78% of global production (Egan et al., 2016; Oraby et al., 2020; Shi, 2024). The process is based on the oxidative dissolution of metallic gold in dilute alkaline cyanide solutions, forming stable aurocyanide complexes. Owing to its selectivity, cost-efficiency, and adaptability to low-grade materials, cyanidation continues to be the principal hydrometallurgical method for gold recovery (Hilson & Monhemius, 2006; Liu et al., 2022).

Low-grade and refractory ores represent more than 30% of global gold reserves and constitute a significant economic resource (Li et al., 2023). In such materials, gold is frequently encapsulated within sulfide minerals such as pyrite, arsenopyrite, and chalcopyrite or occurs as submicroscopic inclusions ("invisible gold"), which significantly hinder direct leaching (Benzaazoua et al., 2007; Chen et al., 2018). Consequently, direct cyanidation of refractory ores often results in low recoveries unless preceded by oxidative pretreatment processes, including roasting, pressure oxidation, or bioleaching, aimed at liberating encapsulated gold particles (Qin et al., 2021; Lin et al., 2022).

The performance of cyanide leaching is governed by a complex interplay of mineralogical, chemical, and hydrodynamic factors. Key operational parameters include particle size distribution, cyanide concentration, dissolved oxygen availability, pulp density, pH, agitation intensity, and leaching duration (Egan et al., 2016; Han et al., 2024; Shi, 2024). Optimization of these variables through controlled experimentation and statistical modeling has been shown to significantly improve gold recovery; for example, Azizi and Ghaedrahmati (2015) achieved 91.5% gold recovery under optimized operational conditions.

Despite its technological maturity, cyanidation poses significant environmental and safety challenges due to the inherent toxicity of cyanide. Maintaining alkaline conditions ($pH > 10.5$) is essential to prevent the formation of hydrogen cyanide (HCN) gas and to ensure process stability (Marsden & House, 2006). Although substantial research has been directed toward alternative lixiviants, including thiosulfate- and glycine-based systems, most alternatives remain at experimental or pilot scale and have not achieved large-scale industrial implementation (Hilson & Monhemius, 2006; Gökelma et al., 2016; Zhang et al., 2022; Wu et al., 2022; Liu et al., 2022).

While the chemistry and operational variables of cyanidation are extensively documented, comparatively limited attention has been directed toward the engineering design and experimental validation of pilot-scale laboratory systems that integrate controlled hydrodynamics, regulated aeration geometry, automated reagent dosing, and long-term operational stability within a single experimental platform. The absence of such integrated systems may restrict the reliability of kinetic modeling and hinder the accurate transfer of laboratory findings to industrial-scale cyanidation circuits.

Accordingly, the present study goes beyond conventional laboratory testing by developing and experimentally validating a pilot-scale cyanidation installation specifically designed to ensure reproducible hydrodynamic conditions, controlled chemical stability, and extended operational performance. The proposed configuration provides a methodological contribution to experimental hydrometallurgy by bridging the gap between small-scale batch testing and industrial process simulation.

Materials and Methods

Design and Construction of the Pilot-Scale Cyanidation System

The pilot-scale laboratory installation for agitated gold cyanidation was designed as an integrated mechanical and process-control platform comprising structural housing, reaction vessels, propeller-type impellers, independent electric drives with inverter regulation, aeration modules, and automated reagent dosing systems. The overall configuration of the unit is presented in Figure 1.

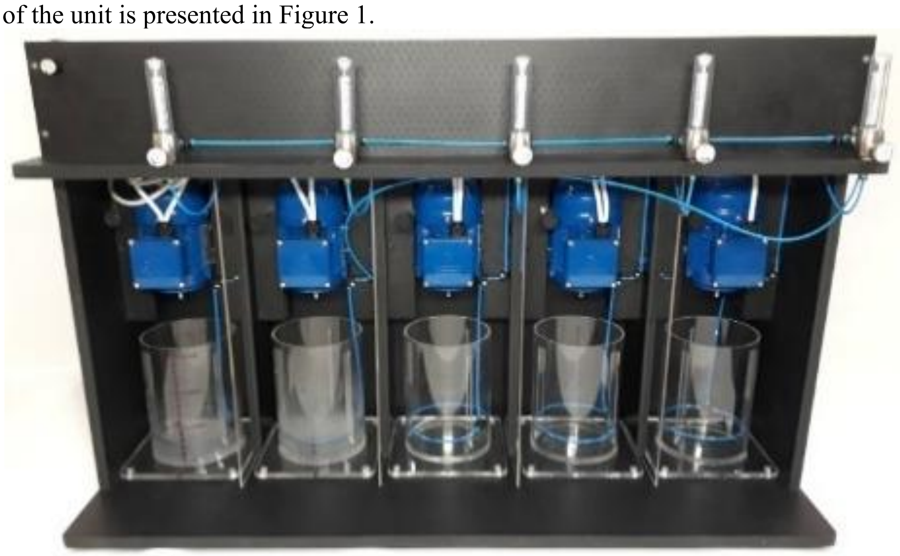

Figure 1. Laboratory equipment

Structural Housing

The main frame of the installation was fabricated from 18 mm hydrophobic multilayer plywood selected for its mechanical strength, abrasion resistance, dimensional stability, and moisture tolerance under prolonged laboratory operation. The system incorporates five independent working stations separated by protective partitions to ensure operational safety and experimental isolation. Each station is equipped with an individual electric motor, enabling independent adjustment of agitation parameters and simultaneous multi-sample testing under controlled conditions.

Reaction Vessels and Agitation System

The reaction vessels were manufactured from polycarbonate (PC), a high-performance transparent polymer characterized by elevated mechanical strength, chemical resistance, thermal stability, and fire-retardant properties. Material selection ensures long-term compatibility with alkaline cyanide media. To provide experimental flexibility for materials of varying gold grades, two reactor volumes were implemented:

- 3000 ml vessels for low-grade ores and tailings,
- 1500 ml vessels for high-grade concentrates.

All vessels are cylindrical and equipped with dual-layer lids incorporating dedicated ports for impeller shafts, reagent addition, aeration, and slurry sampling, enabling closed-system operation with full process accessibility.

Pulp homogenization is achieved through propeller-type impeller assemblies designed to generate intensive hydrodynamic mixing and maintain a fully homogeneous suspension of solid particles. The configuration prevents sedimentation of dense mineral fractions and promotes uniform mass transfer conditions throughout the reactor volume. Reversible rotation capability allows additional control of flow patterns and suppression of vortex formation.

The impellers were fabricated from austenitic stainless steel AISI 316, selected for its mechanical robustness and corrosion resistance under strongly alkaline cyanide conditions. Rotational speed is regulated via inverter-controlled motor drives, permitting precise adjustment of agitation intensity in accordance with hydrodynamic and kinetic requirements.

Aeration System

Aeration was achieved by introducing compressed atmospheric air into the reaction vessels to ensure sufficient dissolved oxygen for the oxidative dissolution of gold. When a specific gaseous environment is required, oxygen or nitrogen may be used instead of air. A series of preliminary trials was conducted to determine the optimal air-injection geometry. The most effective configuration was identified at the vessel periphery, positioned 10 mm below the lower dead center of the impeller. This arrangement enhanced oxygen dispersion, improved gas-liquid mass transfer, and stabilized hydrodynamic conditions without excessive turbulence. Airflow rates were controlled using calibrated glass aerometers (0.1-6 L/min), enabling precise regulation of oxygen supply throughout the leaching process.

Reagent Addition and Process Control

Reagents in aqueous form, including sodium cyanide (NaCN) and pH modifiers, were introduced via peristaltic metering pumps to maintain controlled chemical conditions during leaching. The system supports integration with microprocessor-based control for automated regulation of cyanide concentration and alkalinity. This dosing strategy reduces fluctuations in reagent levels, enhances experimental reproducibility, and minimizes excess reagent consumption. Manual reagent addition via calibrated syringes was retained for short-duration or corrective adjustments.

Slurry Sampling and Monitoring

Slurry samples were collected using disposable tubes (10 ml and 25 ml) connected to a silicone probe integrated into a vacuum-assisted extraction system. This configuration enables representative sampling with minimal disturbance to reactor hydrodynamics. The sampling protocol allows automated periodic collection during long-term experiments of up to 168 hours, supporting continuous process monitoring and reliable kinetic evaluation while limiting operator intervention.

Determination of Gold Recovery and Reagent Consumption

After establishing the optimal grinding fineness of the feed material, a structured experimental program was conducted to determine optimal reagent consumption, including NaCN dosage and pH adjustment requirements. Controlled variation of reagent input allowed identification of concentration ranges that maximize gold dissolution efficiency while limiting unnecessary consumption. Time-dependent leaching experiments were subsequently performed to determine the cyanidation duration corresponding to maximum gold recovery under stabilized chemical and hydrodynamic conditions.

Dissolved gold concentrations were determined by inductively coupled plasma (ICP) analysis following microwave-assisted digestion. Residual gold in solid phases was quantified using fire assay and flame atomic absorption spectrometry in accordance with BDS ISO 10378:2018. The combined analytical approach ensures accurate mass balance evaluation and reliable calculation of gold recovery.

Experimental Conditions

All cyanidation experiments were conducted under controlled laboratory conditions using the pilot-scale installation described above. The feed material was crushed to a particle size below 1.7 mm prior to grinding. The ore was subsequently ground to target fineness levels of P_{60} = 75 µm (i.e., 60% passing 75 µm) and P_{80} = 75 µm for the two experimental series.

Leaching tests were performed at a solids concentration of 40%, using an initial solid mass of 1000 g and a pulp volume of 1500 ml. Agitation was maintained continuously throughout the experiments, and aeration was provided at a controlled airflow rate of 3.0 L/min. The pH of the pulp was maintained above 10.5 to ensure cyanide stability and safe operating conditions.

The total duration of each cyanidation experiment was 48 hours. Incremental additions of sodium cyanide (NaCN) were applied according to the predetermined dosing schedule, resulting in total cyanide consumptions of 2.98 g for the P_{60} = 75 µm test and 2.95 g for the P_{80} = 75 µm test. Lime addition remained constant at 0.37 g in all experiments. Additions of sodium cyanide (NaCN) were applied as needed to maintain its concentration during leaching, resulting in total cyanide consumptions of 2.98 g for the P_{60} = 75 µm test and 2.95 g for the P_{80} = 75 µm test. Sampling was conducted at predefined time intervals using 25 mL slurry aliquots to monitor free cyanide concentration and dissolved gold content.

Results and Discussion

Two experimental series were conducted to evaluate the kinetics of agitated cyanide leaching of the investigated copper-porphyry gold-bearing ore at two grinding fineness levels: P_{60} = 75 µm and P_{80} = 75 µm. The controlled operational parameters, including solids concentration, aeration rate, particle size distribution, and total leaching time, are summarized in Table 1. By maintaining identical process conditions, particle size distribution was effectively isolated as the primary variable influencing gold recovery.

Table 1. Leach test conditions

Parameters	P_{60} = 75 µm	P_{80} = 75 µm
Solids, %	40.0	40.0
Pretreatment	Crushing	Crushing
Crush size, mm	<1.7	<1.7
Leaching time, h	48	48
Air rate, L/min	3.0	3.0
Sample volume, ml	25	25

The cumulative reagent additions applied during the experiments are detailed in Table 2. Total sodium cyanide consumption reached 2.98 g for the P_{60} = 75 µm test and 2.95 g for the P_{80} = 75 µm test, while lime addition remained constant at 0.37 g in both cases. These data indicate comparable cyanide demand under both grinding regimes, despite the differences in recovery behavior.

Table 2. Leach test additions

Leaching time (hr)	P_{60} = 75 µm				P_{80} = 75 µm			
	Solids (g)	Solution (ml)	NaCN (g)	Lime (g)	Solids (g)	Solution (ml)	NaCN (g)	Lime (g)
0	1000	1500	1.50	0.37	1000	1500	1.50	0.37
2	0	1490	0.27	0.00	0	1490	0.25	0.00
4	0	1500	0.30	0.00	0	1490	0.25	0.00
6	0	1490	0.30	0.00	0	1500	0.33	0.00
24	0	1450	0.45	0.00	0	1450	0.46	0.00
30	0	1480	0.16	0.00	0	1480	0.16	0.00
48	0	1440	0.00	0.00	0	1440	0.00	0.00
total	1000	1500	2.98	0.37	1000	1500	2.95	0.37

The evolution of pH, free cyanide concentration, and dissolved gold content throughout the leaching process is presented in Table 3. The pH remained consistently above 10.5, in accordance with established operational practice, thereby ensuring stable alkaline conditions and preventing the evolution of HCN gas (Marsden & House, 2006). The stability of the alkaline environment maintained cyanide in its stable ionic form and minimized reagent loss.

Table 3. Leach test results (solution data)

Leaching time (hr)	P_{60} = 75 µm			P_{80} = 75 µm		
	pH	NaCN (%)	Au (ppm)	pH	NaCN (%)	Au (ppm)
0	10.92	0.100	-	10.92	0.100	-
2	10.90	0.075	0.407	10.90	0.082	0.342
4	10.90	0.128	0.514	10.90	0.119	0.432
6	10.91	0.123	0.560	10.88	0.116	.482
24	10.88	0.062	0.651	10.88	0.062	0.623
30	10.85	0.086	0.666	10.88	0.076	0.610
48	10.83	0.050	0.657	10.85	0.046	0.616
total	10.88	0.089	-	10.89	0.086	-

Leaching Kinetics and Cyanide Availability

The time-dependent dissolution behavior of gold, calculated from solution analyses, is summarized in Table 4 and further quantified in terms of cumulative recovery in Table 5. Gold recovery values were calculated based on mass balance between dissolved and residual gold concentrations determined by ICP and fire assay analysis. The results demonstrate a pronounced initial dissolution phase during the first 6 hours, followed by a progressive deceleration and approach toward a kinetic plateau.

Table 4. Leach test results (sample data)

Leaching time (hr)	P_{60} = 75 µm				P_{80} = 75 µm			
	Volume (ml)	Free CN (mg/L)	Au (µg)	∑ Au (µg)	Volume (ml)	Free CN (mg/L)	Au (µg)	∑ Au (µg)
0	-	540	-	-	-	540	-	-
2	25	405	10.18	10.18	25	445	8.55	8.55
4	25	690	12.85	23.03	25	645	10.80	19.35
6	25	665	14.00	37.03	25	625	12.05	31.40
24	25	335	16.28	53.30	25	335	15.58	46.98
30	25	465	16.65	69.95	25	410	15.25	62.23
48	25	270	16.43	86.38	25	250	15.40	77.63
total	150	481	-	-	150	464	-	-

Maximum gold recovery was achieved after 30 hours of leaching for both grinding conditions, as shown in Table 5. The P_{60} = 75 µm sample reached 75.84% recovery, whereas the P_{80} = 75 µm sample achieved 69.33%. Extending the leaching duration to 48 hours resulted in a slight decrease in recovery, indicating that equilibrium or near-equilibrium conditions were approached within 30 hours under the applied operational parameters.

Table 5. Leach test results (gold data)

Leaching time (hr)	P_{60} = 75 µm			P_{80} = 75 µm		
	Au in Leach (mg/L)	Metal Recovered Au (mg)	Metal Recovered Au (%)	Au in Leach (mg/L)	Metal Recovered Au (mg)	Metal Recovered Au (%)
0	-	-	-	-	-	-
2	606.43	606.43	44.26	509.58	509.58	37.20
4	771.00	781.18	57.02	643.68	652.23	47.61
6	834.40	857.43	62.59	723.00	742.35	54.19
24	943.95	980.98	71.60	903.35	934.75	68.23
30	985.68	1038.98	75.84	902.80	949.78	69.33
48	946.08	1016.03	74.16	887.04	949.27	69.29
total	-	1370.00	-	-	1370.00	-

The evolution of gold recovery as a function of leaching time and grinding fineness is illustrated in Figure 2, which clearly demonstrates the divergence in extraction efficiency between the two particle size distributions after the initial dissolution stage. Correspondingly, the variation in free cyanide concentration during leaching is presented in Figure 3, highlighting periodic cyanide depletion followed by incremental reagent additions that stabilized the chemical environment.

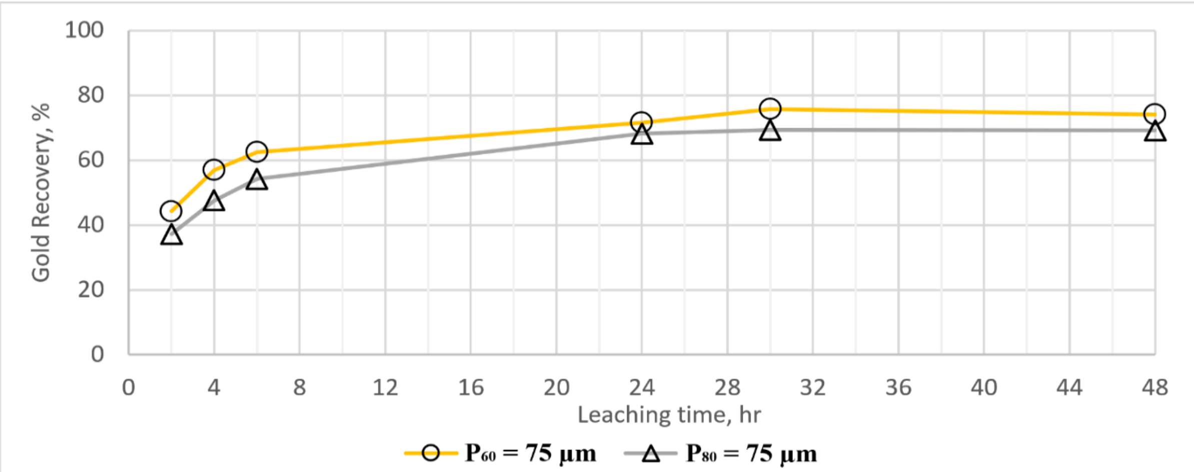

Figure 2. Gold recovery as a function of leaching time

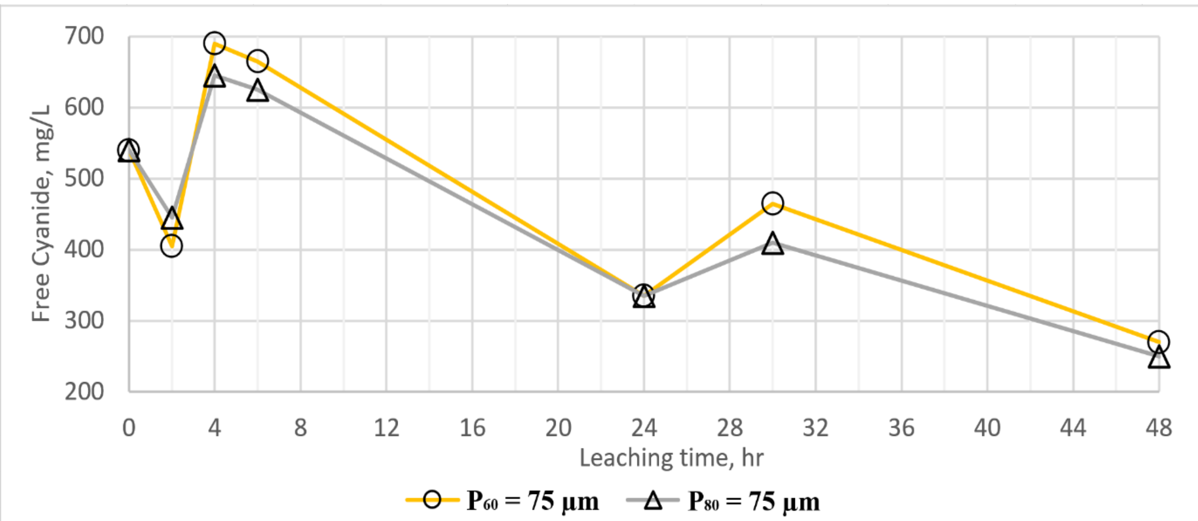

Figure 3. Free cyanide concentration during leaching

The observed kinetic behavior is consistent with diffusion-controlled or surface-reaction-limited dissolution mechanisms reported in cyanidation studies (Egan et al., 2016; Han et al., 2024). The controlled reagent dosing strategy ensured sufficient cyanide availability without excessive overconsumption.

Influence of Grinding Fineness

Although industrial practice often associates finer grinding with enhanced gold recovery due to improved liberation, the present results indicate that excessive size reduction does not necessarily improve gold recovery. Despite the finer particle distribution in the P_{80} = 75 µm sample, the maximum recovery remained lower than that achieved at P_{60} = 75 µm (Table 5).

This behavior may be attributed to overgrinding effects, including increased pulp viscosity and diffusion limitations arising from the formation of fine-grained particles that may act as a passivation layer. Fine particles can adversely affect slurry rheology and reduce effective oxygen mass transfer, thereby diminishing gold dissolution despite the increased surface area.

A comparative summary of maximum gold recovery and reagent consumption is presented in Table 6, which demonstrates that the higher recovery achieved at P_{60} = 75 µm corresponds to slightly more effective cyanide utilization. These findings highlight the necessity of balancing particle size optimization with hydrodynamic and mass transfer considerations.

Table 6. Au recovery and reagent consumption

Parameter	P_{60} = 75 µm	P_{80} = 75 µm
Max. Au Recovery (%)	75.84	69.33
NaCN Consumption (kg NaCN per tonne of ore)	2.98	2.95
Lime Consumption (kg CaO per tonne of ore)	0.37	0.37

Such behavior is consistent with literature reports emphasizing that cyanidation efficiency depends on the coupled interaction of particle size, reagent concentration, oxygen availability, and pH stability rather than on grinding fineness alone (Azizi & Ghaedrahmati, 2015; Egan et al., 2016; Han et al., 2024; Shi, 2024; Banurea et al., 2025).

Process Implications

Overall, the integrated analysis of kinetic data (Tables 4 and 5), reagent consumption patterns (Table 6), and cyanide stability profiles (Table 3; Figure 3) confirms that optimal gold recovery under the investigated conditions was achieved at P_{60} = 75 µm and 30 hours of leaching. The pilot-scale system enabled stable control of hydrodynamic and chemical parameters, thereby generating reproducible data suitable for kinetic modeling and pre-industrial optimization studies.

The consistency of recovery trends across successive sampling intervals, together with the stable pH and free cyanide profiles observed throughout the experiments (Table 3; Figure 3), indicates high reproducibility of the applied methodology. No anomalous fluctuations in dissolution kinetics were detected between the two experimental series, confirming the operational stability and reliability of the pilot-scale installation under controlled hydrodynamic and chemical conditions.

Conclusion

The experimental program confirmed that the designed and commissioned pilot-scale installation for agitated cyanidation provides stable hydrodynamic conditions, controlled reagent dosing, and reproducible operational performance. Under identical leaching parameters, maximum gold recovery was achieved after 30 hours, with superior extraction efficiency observed at P_{60} = 75 µm compared to P_{80} = 75 µm, highlighting the importance of balanced particle size optimization.

The system enables continuous operation for up to 168 hours, simultaneous testing of five independent samples, and automated monitoring with minimal operator intervention. These features ensure high experimental reliability and reduce variability associated with manual process control. The obtained results demonstrate that gold dissolution efficiency is governed by the coupled interaction of particle size distribution, cyanide availability, aeration conditions, and pH stability. The developed installation provides a robust experimental platform for kinetic evaluation and reagent optimization, with strong potential for extrapolation toward semi-industrial and industrial cyanidation circuits. Overall, the proposed system bridges laboratory-scale experimentation and industrial application, supporting improved process control and technological efficiency in gold hydrometallurgical operations.

Scientific Ethics Declaration

* The authors declare that the scientific, ethical, and legal responsibility for this article belongs to the authors.

Conflict of Interest

* The authors declare that they have no conflicts of interest.

Funding

* This research was funded by Project BG05SFPR001-3.004-0002-C01 under Programme "Education", co-funded by the European Union.

Acknowledgements

* This study was presented as a poster at the International Conference on Basic Sciences and Technology (www.icbast.net), Konya, Türkiye, April 02-05, 2026.

* The authors acknowledge the financial support provided under Project BG05SFPR001-3.004-0002-C01 "Development and improvement of professional and interdisciplinary education in technical and economic sciences and enhancement of the research capacity of the extractive industry through project-based doctoral studies", funded by Programme "Education", co-funded by the European Union.

References

Azizi, A., & Ghaedrahmati, R. (2015). Optimizing and evaluating the operational factors affecting the cyanide leaching circuit of the Aghdareh gold processing plant using a CCD model. *Proceedings of the Royal Society A, 471*(2184).

Badri, R., & Zamankhan, P. (2013). Sulphidic refractory gold ore pre-treatment by selective and bulk flotation methods. *Advanced Powder Technology, 24*, 512–519.

Banurea, A. S. R., Nahdi, S. A., & Wahyuningsih, T. (2025). The effect of cyanide concentration and grinding time in tailings on extraction at PT Agincourt Resources. *Journal of Metallurgical Engineering and Processing Technology, 5*(2), 135–142.

Benzaazoua, M., Marion, P., Robaut, F., & Pinto, A. (2007). Gold-bearing arsenopyrite and pyrite in refractory ores: Analytical refinements and new understanding of gold mineralogy. *Mineralogical Magazine, 71*(2), 123–142.

BDS ISO 10378. (2018). *Copper, lead and zinc sulfide concentrates—Determination of gold and silver—Fire assay gravimetric and flame atomic absorption spectrometric method.*

Chen, Y., Song, C. Y., Li, W., & Cai, L. (2018). Mineralogical characteristics of a micro-fine and low-grade refractory gold ore. *MATEC Web of Conferences, 142*, 1–6.

Egan, J., Bazin, C., & Hodouin, D. (2016). Effect of particle size and grinding time on gold dissolution in cyanide solution. *Minerals, 6*(3), 68.

Gökelma, M., Birich, A., Stopic, S., & Friedrich, B. (2016). A review on alternative gold recovery reagents to cyanide. *Journal of Materials Science and Chemical Engineering, 4*, 8–17.

Han, J., Dai, S., Deng, J., Que, S., & Zhou, Y. (2024). Technology for aiding the cyanide leaching of gold ores. *Separations, 11*, 228.

Hilson, G., & Monhemius, A. J. (2006). Alternatives to cyanide in the gold mining industry: What prospects for the future? *Journal of Cleaner Production, 14*(12–13), 1158–1167.

Jaramillo, S. J. N., & Zuñiga, R. E. G. (2025). Characteristics of mineralization of refractory gold and its influence on cyanide gold leaching rates: A case study in Pituca II, Zamora Chinchipe, Ecuador. *Minerals, 15*, 523.

Li, J., Yang, H., Zhao, R., Tong, L., & Chen, Q. (2023). Mineralogical characteristics and recovery process optimization analysis of a refractory gold ore with gold particles mainly encapsulated in pyrite and arsenopyrite. *Geochemistry, 83*(1), 125941.

Lin, Y., Hu, X., Zi, F., Chen, Y., Chen, S., Li, X., Li, J., Jiang, Y., & Zhang, Y. (2022). Rapid gold cyanidation from a sulfur-high and arsenic-high micro-fine concentrate via facile two-stage roasting pre-treatment. *Minerals Engineering, 190*, 107938.

Liu, Z. W., Guo, X. Y., Tian, Q. H., & Zhang, L. (2022). A systematic review of gold extraction: Fundamentals, advancements, and challenges toward alternative lixiviants. *Journal of Hazardous Materials, 440.*

Marsden, J. O., & House, C. I. (2006). *The chemistry of gold extraction* (2nd ed.). Littleton, CO: SME.

Oraby, E. A., Eksteen, J. J., & O'Connor, G. M. (2020). Gold leaching from oxide ores in alkaline glycine solutions in the presence of permanganate. *Hydrometallurgy, 198*, 105527.

Qin, H., Guo, X., Tian, Q., Yu, D., & Zhang, L. (2021). Recovery of gold from sulfide refractory gold ore: Oxidation roasting pretreatment and gold extraction. *Minerals Engineering, 164*, 106822.

Shi, A. (2024). Review of gold cyanide leaching and the main factors affecting gold dissolution rate. *Naturalis Scientias, 1*(1), 56–60.

Wu, J., Ahn, J., & Lee, J. (2022). Characterization of gold deportment and thiosulfate extraction for a copper-gold concentrate treated by pressure oxidation. *Hydrometallurgy, 207*, 105771.

Zhang, Y., Cui, M., Wang, J., Liu, X., & Lyu, X. (2022). A review of gold extraction using alternatives to cyanide: Focus on current status and future prospects of the novel eco-friendly synthetic gold lixiviants. *Minerals Engineering, 176*, 107336.

Author(s) Information

Nikolay Nestorov
University of Mining and Geology "St. Ivan Rilski"
Prof. Boyan Kamenov Str., Sofia, Bulgaria
ORCID iD: https://orcid.org/0009-0008-6543-8771
*Contact e-mail: *n.nestorov@mgu.bg*

Irena Grigorova
University of Mining and Geology "St. Ivan Rilski"
Prof. Boyan Kamenov Str., Sofia, Bulgaria
ORCID iD: https://orcid.org/0000-0002-8243-6232

*Corresponding author(s) email

To cite this article:

Nestorov, N. & Grigorova, I. (2026). Pilot-scale laboratory equipment for agitated gold cyanidation. *The Eurasia Proceedings of Science, Technology, Engineering and Mathematics (EPSTEM), 40,* 184-192.